

Two-layer hierarchical wavelength routing for islands of transparency optical networks

Wenji Wu ^{*,1}, Natalia Gaviria, Kevin M. McNeill, Mingkuan Liu

Computer Engineering Research Laboratory, Electrical and Computer Engineering Department, The University of Arizona, Tucson, AZ 85721-0104, USA

Available online 15 May 2006

Abstract

Although significant advances have been achieved towards the deployment of all-optical networks, optical–electrical–optical (OEO) regeneration is still required due to the lack of proper all-optical processing and all-optical buffering. In order to have a practical, reliable, and cost effective optical transport network, the combination of both all-optical and OEO technologies is necessary. The “islands of transparency” network architecture has been proposed as a solution. This paper presents a two-layer hierarchical wavelength routing (THWR) protocol for the island of transparency optical network. The proposed THWR is a link state protocol that uses a two-layer hierarchy that partitions the network into routing areas, each of which represents an island of transparency. The proposed THWR implements a dynamic wavelength routing capability to balance the network load and avoid the congested area automatically. The complexity analysis and the simulation results of THWR are shown in the paper. The results show THWR is an effective protocol that meets the requirements for optical networks.

© 2006 Elsevier B.V. All rights reserved.

Keywords: Island of transparency; Optical networking; Hierarchical routing; RWA

1. Introduction

Since the 1990s, optical transport networks have been established as the preferred means to transmit digital signals over long distances to create very high capacity networks. Optical communications technology based on DWDM has been hailed as the ideal means to combat data traffic explosion and promises to deliver terabits of raw bandwidth capacity. Hence, with the introduction of more advanced optical device technology, such as EDFA amplifiers, tunable lasers, and tunable add-drop multiplexers, optical communication has moved from a point-to-point transmission topology system, to a more flexible, dynamic, configurable, and manageable network [1,2]. In the technological migration from transmission to

networking, the optical networks are desirable to be both protocol and bit-rate independent. Since all-optical (transparent) networks can offer protocol-independent and bit-rate-independent services, the telecommunications industry is now moving towards an all-optical core network. However, the optical signal is analog, and hence it is affected by various physical impairments that limit the optical reach of the links, i.e. the maximum distance between two points without regeneration [3,4]. Furthermore, due to the lack of proper optical processing and buffering, electronic technology is still required to perform monitoring (e.g., loss of light), assurance to service guarantees (bit error rate of optical connections), error detection/correction, and regeneration. For these reasons OEO (optical–electrical–optical regeneration) is still widely adopted in the current optical transport networks, despite that facts that (1) OEO technology has become costly and power consuming as the bit transmission rate becomes faster, especially at a rate over tens of gigabits; (2) OEO technology cannot offer bit-rate-independent

^{*} Corresponding author. Tel.: +1 6308404541; fax: +1 6308408208.
E-mail addresses: wenji@fnal.gov (W. Wu), mingkuan@email.arizona.edu (M. Liu).

¹ The author is now with Fermi National Accelerator Lab, USA.

and protocol-independent services. Thus, in order to have a practical, reliable, and cost effective optical transport network, the combination of both all-optical and OEO technologies is a necessity.

Currently the widely investigated optical transport network has three types of structures: an all-opaque network, a translucent network and islands of transparency optical network. An all-opaque network, in which the transmission is performed in the optical domain whereas the signal processing takes place in the electrical domain, is consisting of opaque routers. Within each opaque router, the received optical signal is converted to an electrical signal, processed, and then converted back to an optical signal for transmission. The “translucent network” [5,6], on the other side, is formed by hybrid routers [7] which have both all-optical and OEO functionalities. The optical signal goes through OEO conversion when regeneration is needed. Otherwise, the optical signal passes through the hybrid router transparently. The third type of structure, “Islands of transparency” is a network formed by organizing the all-optical routers into subnets, which are interconnected with opaque (OEO) routers to form a larger network [8]. Even though from the signal quality perspective an all-opaque network would be the first choice, it is important to notice that this approach is too expensive and is bit-rate and protocol dependent. The hybrid router network provides good flexibility but requires complex management protocols and has also a very high cost. Furthermore, it exhibits technology actualization issues: if the network needs to provision a new service with a different protocol or bit-rate, all of the routers have to be upgraded to support it. The third approach (islands of transparency) is easier to manage, cost-effective, and more scalable. When new services need to be provided, only the opaque routers are required to be replaced or updated. Islands of transparency optical networks have attracted the interest of academic researchers as well as industry carriers [8].

This new architecture, however, has also raised the need to develop suitable routing protocols that match its

features. One of examples of this trend is the current research aiming at suiting OSPF [9] for optical networks. Since OPSF is designed for packet-switched data networks, some researchers are currently working on extensions to the OSPF in support of wavelength routed optical networks [7,10,11]. Another approach is to build a new routing protocol. In this paper, a two-layer hierarchical wavelength routing protocol (THWR) is developed for the islands of transparency optical network. Similar to traditional routing and wavelength assignment (RWA) heuristic algorithms used in optical networks [12–14], THWR separates the route searching and wavelength assignment problems. The proposed THWR is a hierarchical link state protocol that partitions the optical network into routing areas, each of which constitutes a transparency island. The proposed THWR has dynamic wavelength routing capability to avoid the congested areas automatically. The remainder of the paper is organized as follows: in Section 2 the island of transparency network architecture is presented. Section 3 presents the THWR protocol in detail, and Section 4 present an analysis of the complexity of the proposed algorithm. In Section 5, we show the simulation results to analyze the performance of THWR. Section 6 finally concludes the paper.

2. Island of transparency optical network architecture

Fig. 1 shows the “islands of transparency” optical transport network architecture, which consists of three types of routers: opaque router (OR), all-optical router (AOR) and edge router (ER). “Islands of transparency” are interconnected with opaque routers. All-optical routers reside within the internal core of each island. The edge router has the OE and OE capabilities to collect and deliver the electronic traffic to the edge networks. The size of the islands of transparency is determined by how fast impairments accumulate. It should be chosen so that the optical paths within each island provide acceptable quality of service (e.g. BER). Meanwhile, to

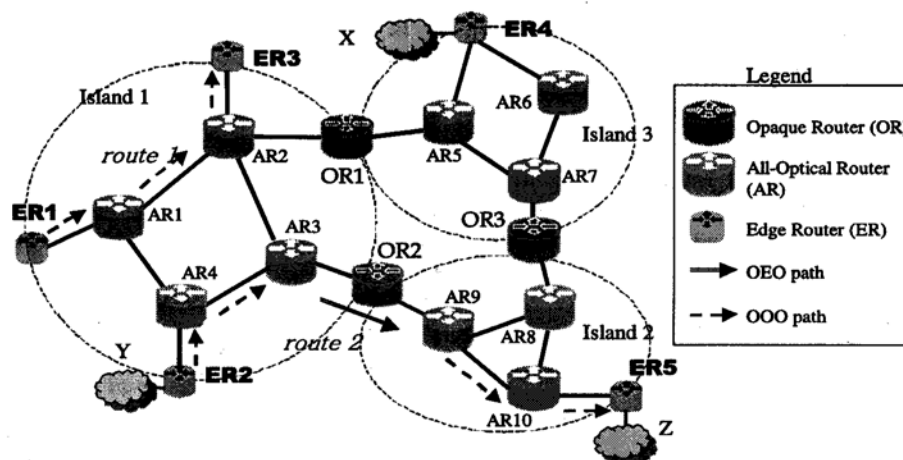


Fig. 1. “Islands of Transparency” optical network architecture.

guarantee connectivity, each island of transparency should be designed in such a way that there is at least one all-optical path with acceptable quality of service between any nodes within the island. Access networks X , Y , Z are connected to the optical network through edge routers (e.g. ER4, ER2 and ER5). In the network, adjacent optical routers are connected by bi-directional, point-to-point DWDM links [15].

The proposed optical network offers the “transparent circuit service”: optical connections are established explicitly end-to-end between edge routers. There are two types of optical connections: (1) Intra-island-all-optical-path: both ingress and egress edge routers belong to the same island. This case is illustrated by route 1 shown in Fig. 1. (2) Inter-island-OEO-path: The ingress edge router and the egress edge router are geographically far away and belong to different islands. OEO regeneration at the intermediate opaque router is needed to eliminate the undesirable optical transmission impairments, as illustrated by route 2 in Fig. 1.

Each individual optical router in the proposed islands of transparency optical network is controlled and managed by the control plane [2,16–19], which comprises two major components: routing protocol and signaling protocol. The routing and signaling protocols are mainly responsible for establishing and tearing down optical connections automatically.

3. Two-layer hierarchical wavelength routing protocol (THWR)

The goal of this section is to model the proposed routing algorithm in the framework of graph theory [20,21]. The first part of this section introduces the necessary definitions to model the network, followed by the specific model of the proposed protocol.

3.1. Hierarchical graph model

$G=(V,E)$ is a directed connected graph, where $V=\{v_i\}$, $i=1:n$ is the set of nodes and $E=\{e_{(i,j)}\}$, $i \in (1:n), j \in (1,n)$ is the set of edges. $e_{(i,j)}$ represents the edge from node v_i to v_j in graph G , where $v_i \in V$, $v_j \in V$, $e_{(i,j)} \in E$. Each node and edge in G has an associated weight to it: $W_{(i,j)}^e$ denotes the weight of edge $e_{(i,j)}$: $0 \leq W_{(i,j)}^e \leq \infty$, and $W_{(i)}^v$ denotes the weight of node v_i : $W_{(i)}^v \geq 0$. In graph G , a path $P_G(i,j)$ is an alternating sequence of nodes and edges, of the form $(v_i, e_{(i,i+1)}, v_{i+1}, \dots, v_{j-1}, e_{(j-1,j)}, v_j)$, where the weight of the path is defined as: $W(P_G(i,j)) = \sum_{k=i}^{j-1} W_{(k,k+1)}^e + \sum_{k=i+1}^j W_{(k)}^v$. Two paths with the same source and destination are different, if their sequences of nodes and edges are different. There might be multiple paths between v_i and v_j in graph G . $Paths_G(i,j) = \{P_G^1(i,j), \dots, P_G^m(i,j)\}$ is the set of all the paths from node v_i and v_j in graph G . $\|Paths_G(i,j)\|$ denotes the number of paths in the path set. In $Paths_G(i,j)$, the path with minimum weight is called the *shortest path*, which is

denoted as $SP_G(i,j)$; if there is no path from node v_i to v_j , then there are $\|Paths_G(i,j)\| = 0$, and $W(SP_G(i,j)) = \infty$.

Definition 1. A *fragment* $F_f=(V_f,E_f)$ of a graph $G=(V,E)$ is a graph, where $V_f \subseteq V$, $E_f \subseteq E$, f is an arbitrary real number. A fragment of G is also a graph that consists of a subset of nodes and edges of G . A *partition* $P = \{F_{f_1}, F_{f_2}, \dots, F_{f_n}\}$ of G , where f_1, f_2, \dots, f_n are arbitrary real numbers, is a set of fragments in G satisfying the following conditions:

- $V_{f_1} \cup V_{f_2} \cup \dots \cup V_{f_n} = V$
- $E_{f_1} \cup E_{f_2} \cup \dots \cup E_{f_n} = E$
- For any two fragments F_{f_i}, F_{f_j} within partition P , $f_i \neq f_j$, $f_i, f_j \in \{f_1, f_2, \dots, f_m\}$ $E_{f_i} \cap E_{f_j} = \phi$;

From this definition it is clear that the same node can be within different fragments; whereas an edge can only exist within one fragment.

Definition 2. Given a partition $P = \{F_{f_1}, F_{f_2}, \dots, F_{f_n}\}$ of graph G , the node intersection of a fragment F_{f_i} with all other fragments of P together is called the *Border Node* (BN) set for F_{f_i} . It is defined as: $BN(F_{f_i}) = V_{f_i} \cap (\bigcup_{f_j \in \{f_1, f_2, \dots, f_m\} \setminus f_i} V_{f_j})$, where $f_j \in \{f_1, f_2, \dots, f_m\} \setminus f_i$. A border node of a fragment appears at least in another fragment of the same partition.

Definition 3. In graph $G=(V,E)$, for any two nodes $v_i, v_j \in V$, if $\|Paths_G(i,j)\| > 0$, then graph G is *connected*. Given a partition $P = \{F_{f_1}, F_{f_2}, \dots, F_{f_n}\}$ of graph G and a fragment $F_{f_i} \in P$, after removing all of its border nodes and their corresponding edges, if the reduced fragment is still *connected*, we say that fragment F_{f_i} is *internally connected*.

Theorem 1. Let us assume a partition $P = \{F_{f_1}, F_{f_2}, \dots, F_{f_n}\}$ of graph $G=(V,E)$, where each fragment is *internally connected*. Given two nodes $v_i, v_j \in V$, v_i and v_j are not both border nodes. If the weight of each border node is assigned big enough, the following two results hold:

- (1) If v_i and v_j belong to the same fragment F_{f_i} , then the shortest path between v_i and v_j in graph G is totally within F_{f_i} , which implies the shortest path's nodes are all from F_{f_i} , and there are no intermediate border nodes.
- (2) If v_i and v_j belong to different fragments, then the shortest path between v_i and v_j in graph G will pass through as few intermediate border nodes as possible.

Please refer to Appendix A for proof details.

Definition 4. Given a partition $P = \{F_{f_1}, F_{f_2}, \dots, F_{f_n}\}$ of $G=(V,E)$, and a node set $V_{sub} \subseteq (V \setminus \bigcup_{f_j} BN(F_{f_j}))$, where $f_j \in \{f_1, f_2, \dots, f_m\}$. A *supergraph* of G is defined as $G^s=(V^s, E^s)$, where: $V^s = (\bigcup_{f_j} BN(F_{f_j})) \cup (V_{sub})$ is the node set of the supergraph. The weight of each node in the

supergraph is 0. $E^s = \{e_{(i,j)}^s | (v_i, v_j) \in V^s\}$ is set of edges of the supergraph. In the supergraph, an edge $e_{(i,j)}^s$ exists between node v_i and v_j , if and only if, $\exists f_i \in \{f_1, f_2, \dots, f_m\}$, $\|SET(P_{F_{f_i}}(i, j))\| \neq 0$, and its weight is defined as $SW^e(i, j) = \min_{f_i} \{SP_{F_{f_i}}(i, j)\}$, $f_i \in \{f_1, f_2, \dots, f_m\}$.

Intuitively, the supergraph of a partition $P = \{F_{f_1}, F_{f_2}, \dots, F_{f_n}\}$ consists of all the border nodes and a designated set of $V_{sub} \subseteq (V \setminus \bigcup_{f_j} BN(F_{f_j}))$, which is a special subset of V without border nodes. The nodes within the set V_{sub} might be chosen by some special criteria. For any nodes $v_i, v_j \in V^s$, If both v_i and v_j exist in a fragment F_{f_i} , and v_j is reachable from v_i to v_j within F_{f_i} , then there is an edge from v_i to v_j in the supergraph, whose weight is the minimum path weight of the shortest paths among all the fragments, which have paths from v_i to v_j .

Theorem 2. Given a partition $P = \{F_{f_1}, F_{f_2}, \dots, F_{f_n}\}$ of graph G , the super graph $G^s = (V^s, E^s)$ of the partition P and a designated node set $V_{sub} \subseteq V \setminus \bigcup_{f_j} B(F_{f_j})$, where $f_j \in \{f_1, f_2, \dots, f_m\}$. For any pair of nodes $v_i, v_j \in V^s$, $W(SP_G(i, j)) = W(SP_{G^s}(i, j))$.

Proof. In [21], JING et. al. have proven similarly for a two-layer model, please refer for details. \square

Definition 5. A two layer hierarchical model of graph $G = (V, E)$ is defined as $LAYER(G) = \{LER_0, LER_1\}$, where the first layer LER_0 is the partition $P = \{F_{f_1}, F_{f_2}, \dots, F_{f_n}\}$ of graph G . The second layer LER_1 is the super graph $G^s = (V^s, E^s)$ constructed as specified in Definition 4.

Corollary 1. Given a two-layer hierarchical model of $LAYER(G) = \{LER_0, LER_1\}$, as specified in Definition 5. For any $SP_{G^s}(i, j)$ in LER_1 with $W(SP_{G^s}(i, j)) \neq \infty$, it is easy to find a corresponding shortest path $SP_G(i, j)$ in LER_0 , where $W(SP_G(i, j)) = W(SP_{G^s}(i, j))$.

Proof. First, locate the corresponding super nodes of $SP_{G^s}(i, j)$ in LER_0 ; then, for each superedge of $SP_{G^s}(i, j)$, find its corresponding shortest path in each related fragment in LER_0 . Hence, when connecting all the shortest paths in each related fragments in LER_0 , a path $P_G^1(i, j)$ in LER_0 is established. Based on Definition 4, we have $W(P_G^1(i, j)) = W(SP_{G^s}(i, j))$. From Theorem 2, we know that $P_G^1(i, j)$ is the shortest path in Layer 0. Then $SP_G(i, j)$ is found. \square

3.2. THWR protocol network graph model

The introduction of hierarchy is one of the key solutions to address network scalability problems [22–26]. THWR is based on the two-layer hierarchical graph model presented in Section 3.1.

In this model, each router is modeled as a node, and each link in the network is represented as two directed edges in opposite directions. The whole optical network is partitioned into fragments based on islands of transparency; each fragment represents an island of transparency.

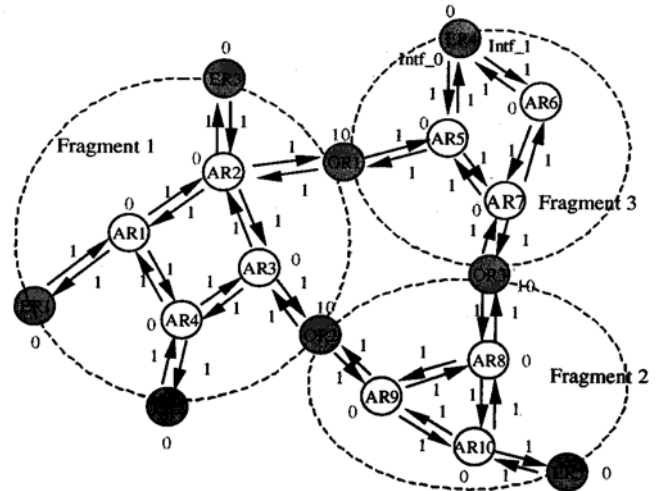


Fig. 2. Graph diagram of an island of transparency optical network.

This set of fragments constitutes the lower layer of the model. The opaque routers constitute the set of border nodes (BN), specified in Definition 2. The edge routers, on the other side constitute the subset V_{sub} , mentioned in Definition 4. Since each island of transparency is designed in such a way that there is at least one all-optical path between any nodes within the island, each fragment is internally connected.

The layer 1 is constructed as a supergraph $G^s = (V^s, E^s)$, where $V^s = \{ER_i, OR_i\}$, such that $ER_i \in V$, $OR_i \in V$. The nodes in the supergraph are the opaque routers (BN) and the edge routers (V_{sub}). Definition 4 determines the conditions to construct the supergraph: if two super nodes from the same island are connected, then there is a superedge between them, and hence a link in the upper layer. In the island of transparency optical network, ORs and ERs usually account for a small portion of the whole network. The Layer 1 network is hence much smaller than Layer 0. Most important of all, the Layer 1 network has the abstracted global network information about the optical network. Figs. 2–4 illustrate the two-layer hierarchical model for the optical network in Fig. 1. Fig. 2 shows the Layer 0 model, which has been partitioned into three fragments based on the islands of transparency. For illustration purposes, weights have been assigned to nodes and edges. In real operations, weights are assigned using a scheme that will be discussed later. Fig. 3 shows super graph of Layer 0 that constitutes Layer 1 in the model. Fig. 4 illustrates the graph model corresponding to the two-layer hierarchical optical network.

3.3. THWR protocol implementation

THWR is a hierarchical link-state routing protocol, and as such it floods Link State Advertisements (LSAs) to build

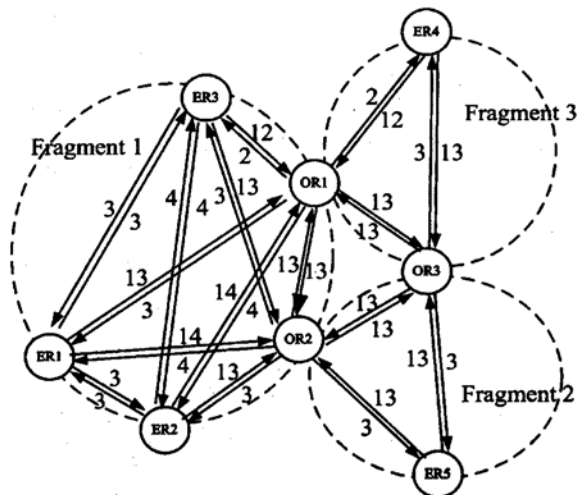


Fig. 3. Supergraph of transparency island partition.

the two-layer hierarchical graph model within routers. THWR originates two types of LSAs: Normal LSA (NLSA), and Super LSA. NLSAs are flooded and restricted within each island to develop the Local Area Routing Tables (LART), and SLSAs are flooded across the whole

network to develop the Global Area Routing Tables (GART).

An optical router (ER, OR, and ER) will originate and flood NLSAs whenever it detects significant events in its outgoing links (e.g. optical link's powering up and down, or a considerable change of available (free) wavelengths in one of its outgoing links). The NLSA is a unit of data describing the local state of the router (router ID, island ID, router type, node weight, etc.) and its connections to adjacent routers in the same island of transparency (e.g. link's bit rate, cost, number of unreserved wavelength, and the adjacent router ID). For each particular router within an island of transparency, the collection of NLSAs from all routers in the island forms the local link state database, from which the LART is built. The router builds a tree to find the shortest path to the other routers in the island. If a router (e.g. OR) might belong to multiple islands of transparency, it would have multiple LARTs. As it was mentioned before, the optical impairments are cumulative and hence increase with the number of nodes in a specific path. Even though the size of the islands of transparency is chosen to guarantee the quality of service, and additional mechanism is added to avoid this problem: when the number of hops in the shortest path is above a limit, the router chooses the next shortest path in the tree,

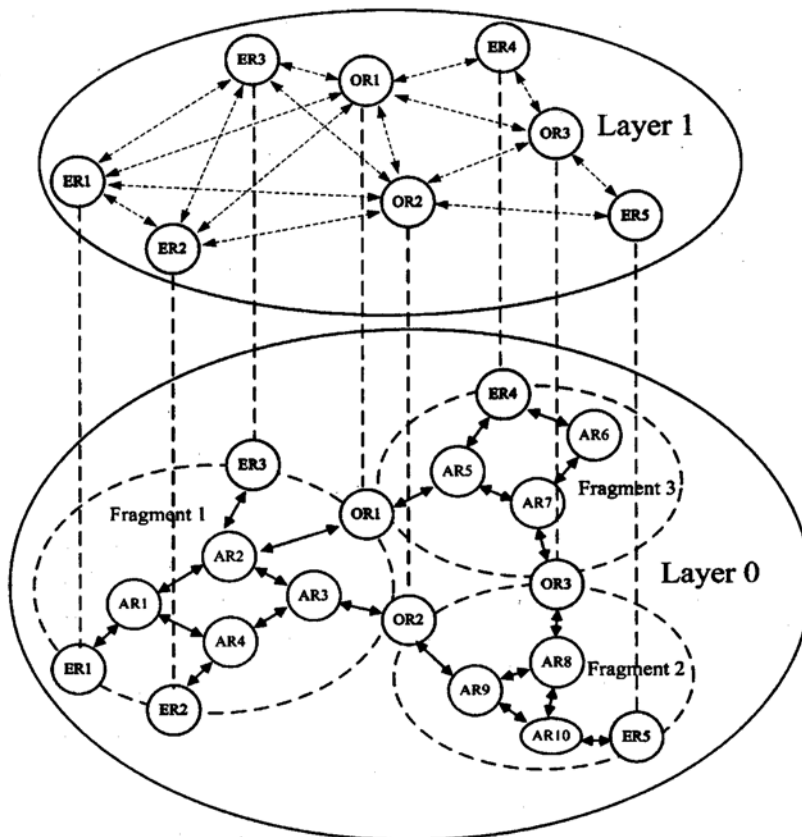


Fig. 4. Two-layer hierarchical graph model.

Table 1
LART at ER4

Dest	Route	Cost	Outgoing Intf
AR5	ER4-AR5	1	Intf_0
AR6	ER4-AR6	1	Intf_1
AR7	ER4-AR5-AR7	2	Intf_0
AR7	ER4-AR6-AR7	2	Intf_1
OR1	ER4-AR5-OR1	12	Intf_0
OR3	ER4-AR5-AR7-OR3	13	Intf_0
OR3	ER4-AR6-AR7-OR3	13	Intf_1

Table 2
GART at ER4

Dest	Route	Cost
ER1	ER4-OR1-ER1	15
ER2	ER4-OR1-ER3	16
ER3	ER4-OR1-ER3	14
ER5	ER4-OR3-ER5	16

given that it has less number of routers. This process is repeated until a suitable path is found.

THWR's Layer 1 graph model is constructed by the SLSAs generated by ERs and ORs. SLSAs are propagated by the ARs, ERs and ORs, but are only processed by ERs. SRLSAs are originated and flooded when ERs/ORs rebuild their local area routing tables. An ER's SRLSA includes its "super edges" (shortest path) to border routers or other ERs in its own island; whereas an OR's SRLSA contains its "super edges" to other ORs and ERs in the islands it belongs to. Based on the information provided by all the SLSAs, GARTs are built in each ER.

Both LARTs and GARTs are rebuilt periodically with the period of Routing Table Rebuilding Interval (*RTRI*). Tables 1 and 2 show an example of LART and GART built at ER4 for the network in Fig. 2.

3.3.1. Routing with THWR

In THWR, optical connections are established along the shortest path between edge routers. Routing takes place during the optical connection establishment phase. Once the optical connection is established, data traffic will tunnel through the established circuit connection, and no further routing is needed. It is the ingress edge router that initiates the connection establishment process. THWR has two types of routing: intra-area routing, and inter-area routing. Intra-area routing takes place when the two ends of the connection belong to the same island. When the connection's source and destination are in different islands, inter-area routing is performed.

In the case of intra-area routing, the ingress edge router looks up its LART, since it includes the strictly explicit route from source to destination within the same island; the signaling messages will follow the route hop-by-hop to set up the connection.

As implied by Corollary 1, an optical connection established along the shortest path in Lay 1 can find a corresponding optimum path in Lay 0. As for the inter-area routing process, the ingress edge router first looks up its

GART to get the *Loosely Explicit Global Route* (LEGR) from source to destination. Since LEGR only specifies the intermediate super nodes, the ingress edge and each intermediate super node need to further search their LARTs to obtain the *Strictly Explicit Local Routes* (SELRs) between adjacent super nodes in the route. For example, to establish an inter-area optical connection between network *x* and *y* in Fig. 1, the ingress node ER4 will first check its LART to select the inter-area routing mechanism. Then, ER4 looks up its GART to get the loosely explicit global route (**ER4-OR3-ER5**) for the connection. After that, ER4 looks up its LART, obtaining the SELR (**ER4-AR5-AR7-OR3**) for route from ER4 to OR3. ER4 inserts the SELR into the global route, and sends out the connection setup message, specifying the source route by (**ER4-AR5-AR7-OR3-ER5**). The connection setup packet follows the source route specified in the message all the way to the next border node OR3. Next, OR3 will in turn look up its LART, obtaining the SELR (**OR3-AR8-AR10-ER5**) for the route from OR3 to ER5. Again, OR3 inserts the SELR into the global route, resulting in the route (**ER4-AR5-AR7-OR3-ER5-AR8-AR10-ER5**). Then the connection setup message will continue to follow the route, until it arrives at the destination ER5.

3.3.2. THWR weight assignment scheme

THWR assigns weight to the edges based on the availability of free wavelengths within each edge. THWR uses the following weight function for each edge [27]:

$$w = \begin{cases} \alpha & \lambda = 0; \\ \beta & \lambda = 1; \\ -\alpha * \log(1 - \frac{1}{\lambda}) & \lambda > 1; \end{cases}$$

- (1) λ is the number of free available wavelengths on each edge;
- (2) α , β are positive constants, which should be large enough to differentiate the cost for each edge with different λ s;
- (3) α and β should meet the relations: $\alpha * \log \frac{1}{2} < \beta < \alpha$.

The purpose of dynamic edge weight assignment scheme is to balance the traffic across network and results in less blocking rate.

In THWR, ORs are assigned a high weight (compared with edge weights), whereas the ARs and ERs are assigned a weight of zero. An easy way to assign weight to ORs can be as follows: first, find an island of transparency with the maximum number of optical links, say m links; Then, if the weight assigned to each OR is larger than $a * m$, the conditions specified in Theorem 1 will be met. As proofed in Theorem, this assignment scheme can avoid unnecessary OEO conversions for optical connections, saving the network resources. However, the weight of ORs can be reconfigured for administrative and management purposes. For example, when a specific island of the network is

getting congested, the weight of all the ORs of the island can be increased, to bypass future traffic to other islands.

3.3.3. Wavelength assignment/de-assignment with THWR

The wavelength assignment process takes place when routers receive connection setup signaling messages. So far, THWR adopts a fixed-order wavelength assignment strategy: the first available wavelength will be assigned when needed. Wavelength de-assignment occurs when the router receives the connection tear down signaling messages. The wavelength assignment (de-assignment) process causes available wavelength changes within optical links. To limit THWR protocol overheads, an optical router originates NLSAs whenever it detects a significant change of available wavelengths in one of its outgoing link. Here, the significant change of available wavelength is defined as: $\frac{|W_{avail_prior} - W_{avail_after}|}{W_{Total}} \geq Threshold$, Where, W_{Total} is the total wavelength number for the link; W_{avail_prior} is the number of available wavelengths in the link prior to the change; W_{avail_after} is the number of available wavelengths after the change. *Threshold* is the preset link statement advertisement threshold.

4. Complexity of THWR

Suppose there are N nodes in the optical network. In the regular flat LSR algorithm [28], each node in the network will generate one LSA message and flood it to every other node once. Therefore, the total amount of communication overhead generated by the regular flat LSR is:

$$T_{LSR} = N * (N - 1) \text{ Messages.}$$

To analyze the overhead of THWR, suppose that the optical network is divided into M islands evenly, in which each island has (N/M) nodes. Suppose also that there are K super nodes selected from these islands to construct the super graph. Thus, the communication overhead for the flooding NLSA messages within each island will be $((N/M) * ((N/M) - 1))$, which renders $((N^2/M) - N)$ messages in the whole network. Moreover, each super node in the super graph will generate one SLSA message and flood it across the network. The amount of this type of message is $K(N - 1)$. Therefore, the total amount of communication overhead generated by the proposed THWR is:

$$T_{THWR} = (N^2/M) - N + K * N - K \text{ Messages.}$$

Hence, the proper selection of M and K will lower the overhead of THWR, as compared to regular flat LSR. As a rule of thumb, values of M and K in the range $2 < M, K < N/2$ will result in a better performance of T_{THWR} in terms of overhead, since the flooding communication overheads will be smaller than in the regular flat LSR algorithm.

In the regular flat LSR algorithm, the topology table maintained by each router requires memory storage size of $O(N)$, while in the proposed THWR algorithm, the LART maintained by each router requires memory storage size of $O(N/M)$. As to GART, the table storage size is of $O(K)$.

Therefore, for an opaque or all-optical router, the total required memory storage size will be $O(N/M)$; and for an edge router, the total memory storage required will be in size of $O(N/M) + O(K)$. When values of M and K are in the range $2 < M, K < N/2$, THWR required memory would be saved, especially for all-optical routers. From this analysis, evidently the proposed THWR algorithm consumes less router memory than the regular flat LSR algorithm.

5. Implementation and simulation

The implementation and simulation of the THWR protocol is based on our previous work on GMPLS virtual router, developed on OPNET Modeler²[27]. The optical router's (ER, AR, and OR) control plane consists of the THWR routing module and the RSVP signaling module. The goal of the simulation experiments is to evaluate the performance of our proposed THWR protocol and islands of transparency optical network architecture. The simulation experiments are run with the same network topology³, but with two different network architectures. Fig. 5a shows the simulation network topology, comprising 40 nodes. (a) Fig. 5b illustrates the Opaque Network Architecture. Each router runs OSPF protocol and the whole network is considered as one OSPF routing area. To enable OSPF to run in the optical network context, some optical extensions were added to OSPF, so that every flooded LSA carries information regarding to the total number of wavelengths and the number of unused wavelengths for the corresponding links. (b) Fig. 5c illustrates the architecture used to simulate the islands of transparency scenario. In this case, the whole network is split into four islands of transparency, interconnected by opaque routers. Each router runs THWR protocol.

The following assumptions are made when running the simulations:

- No reattempt to send packets is performed when a connection is blocked.
- Each DWDM link has one fiber; the number of wavelength within each fiber is 10.
- Optical connections are set up and torn down between edge routers.
- Each all-optical router has the full all optical wavelength conversion capability.
- Optical connections set up requirements arrive at edge optical router as a Poisson process with arrival rate λ . If the optical connection is set up successfully, it will keep operating for a t time before it is torn down, where t is a random variable with exponential distribution, with parameter $1/T$. Hence, the traffic load offered to the network is given by $r = T \times \lambda$. In the simulations, t is chosen to be 10 s.

² OPNET Modeler is a Trade Mark of OPNET Technologies, Inc., Bethesda, MD.

³ Similar simulation results have been obtained upon other types of topologies.

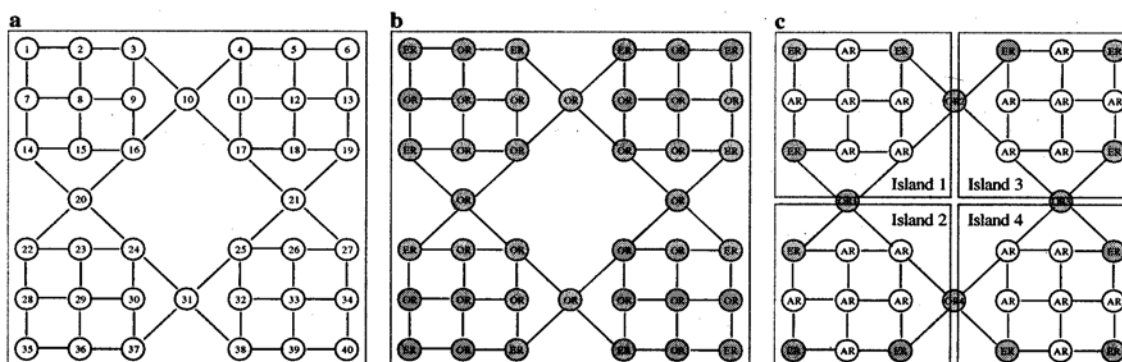


Fig. 5. (a) Simulation topology, network architecture: (b) opaque, (c) islands of transparency.

The performance metrics used in the analysis and evaluation of the algorithm are blocking rate and protocol traffic overheads. The results presented in the following sections are averages across multiple simulation runs. Each point in the plots is an average of 10 runs using different random number seeds.

5.1. Comparison between OSPF and THWR

Since OSPF is the most widely studied routing protocol in optical networks, it is taken as the reference point to evaluate the performance of THWR. Also, to evaluate the effectiveness of the dynamic link weight assignment mechanism discussed in Section 3, we compare it with a static weight assignment scheme. In the static weight assignment scheme, a fixed weight is assigned to each link, not considering its available wavelengths. In the following sections, we specify “D-OSPF” and “S-OSPF” to indicate the OSPF managed Opaque-Optical-Network, with Dynamic and Static weight assignment scheme respectively. Similarly, we denote “D-THWR” and “S-THWR” to indicate the THWR-managed Island-of-Transparency Optical Network with Dynamic and Static weight Assignment Scheme, respectively.

In this scenario, the routing table rebuilding interval and the LSA flooding threshold are kept constant to 60 s and 10%, respectively. In our simulations, an OSPF router has the detailed information about the whole network; whereas a THWR router has only partial network information. Fig. 6 shows the performance of both architectures operating under static and dynamic assignment conditions. It can be observed that the blocking rate in both cases is very similar for a specific type of cost assignment. This means that even though THWR uses partial network information it can be as effective (or some times even more) as OSPF.

Meanwhile, the figure illustrates the effectiveness of the dynamic weight assignment mechanism. The results show a better blocking rate for the dynamic assignment in both cases, especially when the network load is light. When the network traffic load increases, the advantages of

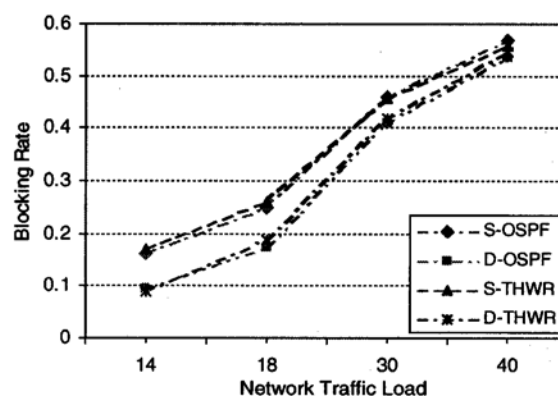


Fig. 6. Blocking rate comparison between OSPF and THWR with static and dynamic assignment.

dynamic link weight assignment scheme over static link weight assignment are not so apparent. This is due to the fact that the dynamic link weight assignment scheme tends to route the optical connection requests across the network by choosing different paths to decrease the blocking rates whereas in the static link cost assignment scheme, the optical connection requests will always take the same paths. When the network traffic is light, more network resources (wavelengths) are available and hence the dynamic link weight assignment scheme will perform much better than the static scheme. On the other hand, when the network traffic load is high, most of the network resources have been occupied, and even in the dynamic scheme it is hard to find a path to route the new optical connection request successfully.

Fig. 7 compares the performance of OSPF and THWR in terms of the protocol traffic overhead, under a dynamic weight assignment scheme. The routing rebuilding interval and LSA flooding threshold are kept constant as in the previous case. The plots show the received LSA traffic at two specific nodes in the network. Fig. 7a illustrates the traffic at node 2. In the opaque network architecture, this node is a normal OSPF router, and hence it receives each originated OSPF LSA in the network. In the island of transpar-

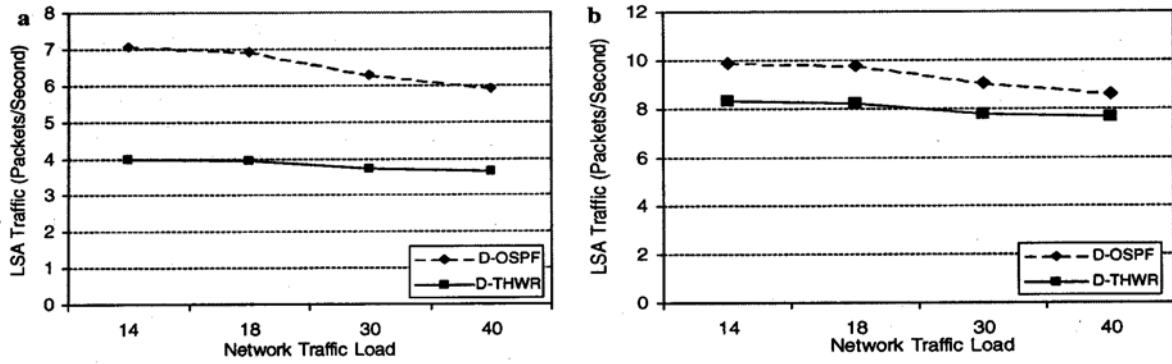


Fig. 7. Protocol traffic overhead comparison between OSPF and THWR at (a) Node 2 and (b) Node 10.

ency network architecture, the same node only receives the NLSA traffic from its own island, and the SLSA traffic from the whole network. Similarly, Fig. 7b illustrates the behavior of Node 10, which represents a normal OSPF router in the opaque network architecture, and constitutes a border router in the islands of transparency configuration (and hence it receives the NLSA traffic from two islands, and the SLSA traffic from the whole network). The results show that the amount of LSA traffic received by both nodes is lower when using the islands of transparency architecture. However, the results also indicate that the border router (Node 10) receives more LSA traffic than a normal THWR router within the island (Node 2), and that the difference

between the two architectures is more pronounced in the case of the internal router (Node 2).

5.2. The routing table interval's effect on the performance of THWR

Both LARTs and GARTs are rebuilt periodically with the period of RTRI. SRLSAs are originated and flooded every time the edge/border routers rebuild their LARTs, and hence the latest network topology and resource changes will be reflected and updated. Fig. 8 shows the simulation results of the effect that the RTRI has on the performance of THWR.

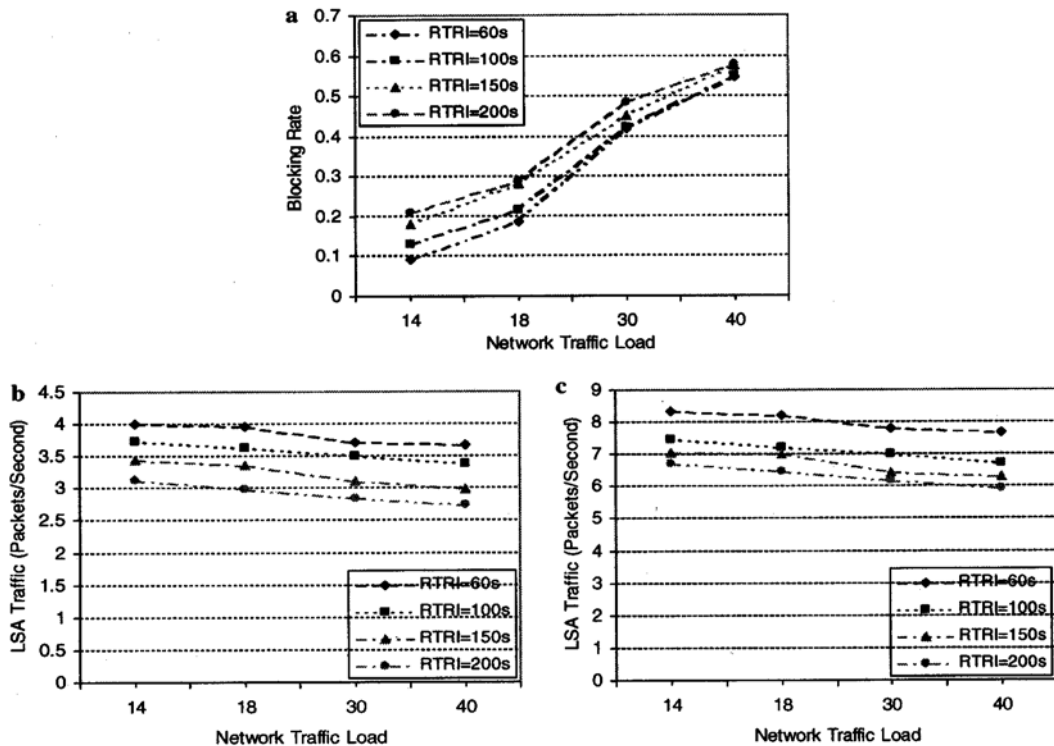


Fig. 8. Effect of the RTRI on the performance of THWR.

Fig. 8a shows the effect of the RTRI on the performance of the network in terms of blocking rate. It can be observed that the performance is heavily affected, especially for light traffic load. When the RTRI increases, the blocking rate increases too. Hence, the lowest blocking rate is obtained for the 60-second-RTRI. For example, at traffic load of 14, the 60-second-RTRI's blocking rate is around 9%; whereas the blocking rate of the 200-second-RTRI is as high as 22%. In terms of traffic overhead, it is expected that smaller RTRI generate more LSA traffic, since the updates are flooded more often. This is verified by the simulation results illustrated in Figs. 8b and c, which show the received LSA traffic at Node 2 and Node 10, respectively. Both figures have demonstrated that with smaller RTRIs, THWR will generate more LSA traffic (SRLSAs).

5.3. LSA flooding threshold effect on the performance of THWR

Another important THWR parameter that requires tuning is the NLSA flooding threshold. Fig. 9 illustrates the effect of the flooding threshold on the performance of the protocol. Fig. 9a illustrates the performance in terms of blocking rate for three different threshold values: 10%, 30% and 80%. The blocking rate increases with the threshold value, as shown in the results. Figs. 9b and c show the impact of the threshold value on the protocol overhead

performance for nodes 2 and 10, respectively. It can be seen that the amount of overhead traffic decreases when the threshold increases. That is, the choice of a specific threshold value is a tradeoff between the blocking rate and the LSA traffic. Once again, it can be observed that the amount of overhead is higher for the opaque router.

6. Conclusions

This paper has presented a new hierarchical link state routing protocol, called THWR, for the islands of transparency optical network. By taking advantage of the characteristics of the islands of transparency network topology, the proposed protocol partitions the whole optical network into routing areas, each of which constitutes a transparency island. Differing from other hierarchical routing protocols, THWR does not require the definition of a backbone routing area, as is the case of OSPF [9], nor does it designate any node as peer group leader as in a hierarchical ATM network [22]. As a result, the proposed protocol is easier to maintain, and more flexible from the perspectives of deployment. Network scalability is a very important design consideration.

Analysis and simulation results show that the amount of communication overhead in the proposed THWR is less than that of flat LSR (e.g., flat OSPF). Meanwhile, the mathematical analysis has also shown that THWR con-

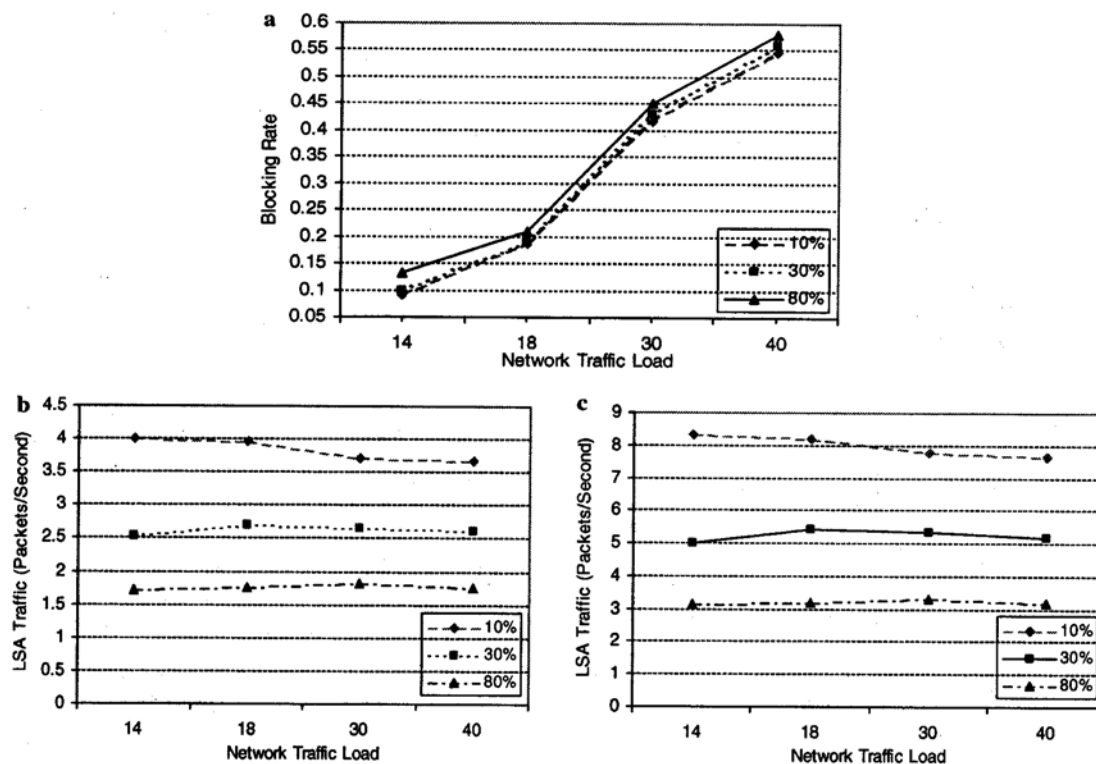


Fig. 9. Effect of the LSA flooding threshold on the performance of THWR.

sumes less router memory than the regular flat LSR algorithm. It is clear then that THWR is more bandwidth efficient and scales better than regular flat LSR. Since THWR is designed purely for optical networks, it takes full considerations of optical network's characteristics. In THWR-managed optical network, unnecessary OEO conversions for optical connections are avoided. Furthermore, THWR adopts the dynamic cost assignment scheme to balance the load across the network, while reducing the blocking probability. As a consequence, THWR-managed optical networks are more economic and efficient.

Appendix A. Proof of Theorem 1

Result (1) Proof. The path set $Paths_G(i, j) = \{P_G^1(i, j), \dots, P_G^m(i, j)\}$, will include all the paths from node v_i and v_j in graph G . There are three types of possible paths with the set:

- Type one: the path consists of nodes only from F_{f_i} , there are no intermediate border nodes.
- Type two: the Path consist of nodes only from F_{f_i} , there are intermediate border nodes.
- Type three: the path consists of nodes from fragments other than F_{f_i} . Apparently this type of path will include intermediate border nodes.

Since fragment F_{f_i} is internally connected, by Definition 3, within fragment F_{f_i} , there is at least a type one path from v_i to v_j in F_{f_i} . Assume it is $P_G^1(i, j) = (v_i, e_{(i,i+1)}, v_{i+1}, \dots, v_{j-1}, e_{(j-1,j)}, v_j)$, apparently $W(SP_G(i, j)) \leq W(P_G^1(i, j))$. If each border node is assigned the same weight, and the weight is larger than $W(P_G^1(i, j)) - W^v(j)$, the weight of any type two or type three path is larger than that of the type one. Thus the shortest path between v_i and v_j in graph G is totally within F_{f_i} , which implies the nodes in the shortest path are all from F_{f_i} . There are no intermediate border nodes, and hence $SP_G(i, j) = SP_{F_{f_i}}(i, j)$. \square

Result (2) Proof. The path set $Paths_G(i, j) = \{P_G^1(i, j), \dots, P_G^m(i, j)\}$ includes all the paths from node v_i and v_j in graph G . Assume $P_G^1(i, j) = (v_i, e_{(i,i+1)}, v_{i+1}, \dots, v_{j-1}, e_{(j-1,j)}, v_j)$ is the path with least intermediate border nodes. If each border node is assigned the same weight, and the weight is larger than $\sum_{k=i}^{j-1} W_{(k,k+1)}^e$, $P_G^1(i, j)$ is guaranteed to be the shortest path between v_i and v_j in graph G . Any other path in $Paths_G(i, j)$ is longer than $P_G^1(i, j)$. \square

References

- [1] R. Ramaswami, Optical Fiber Communication: From Transmission to Networking, in: IEEE Communication Magazine, 50th Anniversary Commemorative Issue, May 2002, pp. 138–147.
- [2] Peter Tomsu, Christian Schmutzer, in: Next Generation Optical Networks: The Convergence of IP Intelligence and Optical Technologies, Prentice Hall PTR, ISBN 0-13-028226-X, 2002.
- [3] J. Strand, A.L. Chiu, R. Tkach, Issues for Routing In the Optical Layer, IEEE Communication Magazine (2001) 81–87.
- [4] R.S. Vodhanel, et al., Post Deadline Paper PD27, OFC '97, Dallas, TX, Feb. 1997.
- [5] B. Ramamurthy, S. Yaragorla, X. Yang, Translucent Optical WDM Networks for the Next-Generation Backbone Networks, in: IEEE GLOBECOM'01, Global Telecommunications Conference, vol. 1, 2001, pp. 60–64.
- [6] A.L. Soliza Filho, H. Waldman, Strategies for designing translucent wide-area networks, Microwave and Optoelectronics Conference, in: Proceedings of the 2003 SBMO/IEEE MTT-S International, vol. 2, 2003, pp. 931–936.
- [7] K. Sato, N. Yamanaka, Y. Takigawa, M. Koga, S. Okamoto, K. Shiimoto, E. Oki, W. Imajuku, GMPLS-based photonic multilayer router (Hikari router) architecture: an overview of traffic engineering and signaling technology, IEEE Communications Magazine 40 (3) (2002) 96–101.
- [8] P. Green, Progress in optical networking, IEEE Communications Magazine 39 (1) (2001) 54–61.
- [9] J. Moy, OSPF Version 2, IETF RFC 2328, April 1998.
- [10] S. Sengupta, D. Saha, S. Chaudhuri, Analysis of enhanced OSPF for routing lightpaths in optical mesh networks, in: ICC 2002. IEEE International Conference on Communications, vol. 5, pp. 2865–2869.
- [11] K. Kompella, Y. Rekhter, OSPF Extensions in Support of Generalized Multi-Protocol Label Switching (GMPLS), Network Working Group, RFC4203, October 2005.
- [12] T.E. Stern, K. Bala, Multiwavelength Optical Networks – A Layered Approach, Prentice Hall, Englewood Cliffs, NJ, 2000.
- [13] R. Ramaswami, K.N. Sivarajan, Routing and wavelength assignment in all-optical networks, IEEE/ACM Transactions on Networking 3 (5) (1995) 489–500.
- [14] D. Banerjee, B. Mukherjee, A practical approach for routing and wavelength assignment in large wavelength-routed optical networks, IEEE Journal on Selected Areas in Communications 14 (5) (1996) 903–908.
- [15] S.V. Kartalopoulos, Introduction to DWDM Technology: Data in a Rainbow, IEEE Press, New York, 2000.
- [16] Guangzhi Li, J. Yates, Dongmei Wang, C. Kalmanek, Control plane design for reliable optical networks, IEEE Communications Magazine 40 (2) (2002) 90–96.
- [17] D. Saha, B. Rajagopalan, G. Bernstein, The optical network control plane: state of the standards and deployment, IEEE Communications Magazine 41 (8) (2003) S29–S34.
- [18] Hui Zang, J.P. Jue, L. Sahasrabudhe, R. Ramamurthy, B. Mukherjee, Dynamic lightpath establishment in wavelength routed WDM networks, IEEE Communications Magazine 39 (9) (2001) 100–108.
- [19] Zhensheng Zhang, James Fu, Dan Guo, Leah Zhang, Lightpath routing for intelligent optical networks, IEEE Network 15 (4) (2001) 28–35.
- [20] Ravindra K. Ahuja, Thomas L. Magnanti, James B. Orlin, Network Flows: Theory, Algorithms, and Applications, Prentice Hall, ISBN 0-13-617549-X, 1993.
- [21] N. Jing, Y.-W. Huang, E.A. Rundensteiner, Hierarchical encoded path views for path query processing: an optimal model and its performance evaluation, IEEE Transactions on Knowledge and Data Engineering 10 (3) (1998) 409–432.
- [22] E. Felstaine, R. Cohen, On the distribution of routing computation in hierarchical ATM networks, IEEE/ACM Transactions on Networking 7 (6) (1999) 906–916.
- [23] J. Sucec, I. Marsic, Hierarchical routing overhead in mobile ad hoc networks, IEEE Transactions on Mobile Computing 3 (1) (2004) 46–56.
- [24] W.T. Tsai, C.V. Ramamoorthy, W.K. Tsai, O. Nishiguchi, An adaptive hierarchical routing protocol, IEEE Transactions on Computers 38 (8) (1989) 1059–1075.
- [25] S. Murthy, J.J. Garcia-Luna-Aceves, Loop-free Internet routing using hierarchical routing trees, in: INFOCOM '97. Sixteenth Annual Joint Conference of the IEEE Computer and Communi-

- cations Societies. Proceedings IEEE, vol. 1, 7–11 April 1997, pp. 101–108.
- [26] Y. Suemura, I. Nishioka, Y. Maeno, S. Araki, R. Izmailov, S. Ganguly, Hierarchical routing in layered ring and mesh optical networks, IEEE International Conference on Communications 5 (2002) 2727–2733.
- [27] R. Martinez, Wenji Wu, P.Y. Choo, The modeling process and analysis of virtual GMPLS optical switching routers, Journal of Photonic Network Communications 8 (1) (2004) 39–54.
- [28] R. Perlman, Interconnections: Bridges and Routers, Addison-Wesley, Reading, MA, 1992, pp. 149–152, 205–233.



Wenji Wu holds a B.A. degree in Electrical Engineering (1994) from Zhejiang University (Hang Zhou, China), M.S in industrial engineering (2001) and doctorate in computer engineering (2003) from the University of Arizona, Tucson AZ. Dr. Wu is currently a Network Researcher in Fermi National Accelerator Laboratory, USA. His research interests include high performance networking, operating systems, wireless networks, optical networking, and modeling and simulation.



Natalia Gaviria was born in Colombia in 1972 and holds a BS degree in Electronics Engineering (1996) from the University of Antioquia, M.S in Electrical Engineering from Los Andes University (2000). She is currently a PhD student at Electrical and Computer Engineering Department at the University of Arizona. Her research interests include Management and Control plane protocols and architectures, Optical Networking, Ad Hoc Networks, and modeling and simulation.



Kevin M. McNeill (M'87) was born in Tucson AZ in 1956 and holds a B.A. in mathematics ('83), M.S in computer science ('87) and doctorate in computer engineering ('93) all from the University of Arizona, Tucson AZ. He is currently the Chief Engineer, Network-centric Systems at BAE SYSTEMS, Network Enabled Solutions, in Reston VA where he is also serving as the Manager of the Advanced Networking Group. He was formerly a Research Associate Professor in the Department of Electrical & Computer Engineering and Acting Director of the Computer Engineering Research Laboratory, University of Arizona. He has held numerous appointments in the College of Medicine, including Associate Research Scientist in the Department of Radiology, and Chief Information Officer and Network Architect for the Arizona Telemedicine Program. He has published extensively on topics related to computer and networking aspects of Digital Radiology and Telemedicine. His current research interests include Network Aware Applications, MANET, optical networking, unified control plane/management plane protocols, sensors networks and data fusion, and modeling and simulation.



Mingkuan Liu is a PhD student in the Electrical and Computer Engineering Department at the University of Arizona. His research interests include speech recognition, web caching, voice over IP, and multimedia delivery over wireless Internet. He received a MS in information science from the Institute of Automation, Chinese Academy of Sciences and a MS in industrial engineering from the University of Arizona in 2000 and 2002, respectively.

